Chitosan modified Pluronic F-127 at SnO_2 NPs Prepared via Green Synthesis Using Sennaauriculata leaf extract and it their Biomedical applications.

1*. Parameswari. P

2. Sakthivelu A

1*. Research Scholar, PG and Research Department of Physics, Thanthai Periyar Government Arts and Science College (Autonomous), Tiruchirappalli – 620 023.Affiliated to Bharathidasan university, Tiruchirappalli,Tamilnadu, India. parameswarinagas@gmail.com

2. Assistant Professor, PG and Research Department of Physics, Thanthai Periyar Government Arts and Science College (Autonomous), Tiruchirappalli – 620 023. Affiliated to Bharathidasan university, Tiruchirappalli,Tamilnadu, India.

Abstract

This study seeks to learn more about SnO_2Pluronic F127 Chitosan Sodium. SnO_2Pluronic F127 Chitosan NPs have been shown to have a tetragonal rutile structure by means of both X-ray diffraction and field-emission scanning electron microscopy. In the FTIR spectra of SnO_2 NPs, the Chitosan functional group and the Pluronic F127 overtone bands are visible, while the characteristic peaks of SnO_2 NPs are located at 619 cm^{-1} in the spectra of SnO. The morphologies of SnO_2PluronicF127 Chitosan were analysed using scanning electron microscopy (SEM). SnO_2Pluronic F127 Chitosan NPs have DLS spectra and hydrodynamic sizes of (169 nm), respectively. Due to oxygen vacancies and other defects, SnO_2Pluronic F127 Chitosan NPs have blue emission peaks in their PL spectra, specifically at 467 nm. Antibacterial activity against *Staphylococcus aureus, Klebsiellapneumoniae, Shigelladysenteriae, Pneumocystis jirovecii, Bacillus megaterium,* and *Proteus valgaris* was reevaluated using the well-diffusion technique using SnO_2Pluronic F127 Chitosan NPs and Amoxicillin. To learn more about how effective nanoparticles are at inhibiting the growth of Candida albicans, they were tested in a well diffusion apparatus. A human breast cancer cell line (MDA-MB-237) was treated with SnO_2 Pluronic F127 Chitosan NPs and exhibited similar anticancer activity. These findings lend credence to the idea that SnO NPs modified

with biopolymers Chitosan and Copolymer Pluronic F127 could have useful applications in healthcare manufacturing settings.

Keywords: Chitosan modified Pluronic F-127; SnO_2; Breast cancer cell line; Antibacterial and Antifungal Activity; Anticancer activity;

*Corresponding author: parameswarinagas@gmail.com

INTRODUCTION

In 2020, there were approximately 19.3 million new cases of cancer worldwide, according to data from the Global Cancer Observatory (GLOBOCAN). India came in at number three, behind only China and the United States. In accordance with GLOBOCAN, the number of cases of cancer in India may rise to 2.08 million by 2040, a 57.5 percent increase from 2020[1-2].

Cancer is a disease characterised by the unchecked proliferation and metastasis of abnormal cells. Since the human body is composed of trillions of cells, cancer can arise virtually anywhere. In a healthy human body, cells divide and multiply to produce new cells as they are needed. Old or damaged cells die, and new ones take their place as the body repairs itself. When this normally controlled process fails, abnormal or damaged cells proliferate when they shouldn't. Tumours, or masses of accumulated tissue, can develop from these cells. Cancer can develop in tumours. It is possible for cancerous tumours to invade neighbouring tissues and metastasize to other parts of the body. Malignant tumours are another name for cancerous tumours. Cancers of the blood, such as leukaemias, rarely develop into solid tumours, in contrast to many other types of cancer. Benign tumours do not metastasize, or spread to other parts of the body. Benign tumours are less likely to return after removal than malignant ones.

However, benign tumours can occasionally reach impressive dimensions. Some, like brain tumours, can cause severe symptoms or even be fatal[3-9].

Unchecked cell proliferation, which is the hallmark of cancer, is caused by mutations in genes that normally control the cell cycle and division. Essentially, this is how cancer forms. However, conventional chemotherapeutic drugs come with a host of problems, such as low bioavailability, rapid renal clearance, erratic dosing, and dangerous side effects. Breast cancer has become the leading cause of death for women worldwide in recent years. By the year 2030, 13.1 million people will have died from these illnesses, according to the World Health Organisation.

Worldwide, breast cancer is the most common form of the disease among females of reproductive age. It's a malignancy wherein the breast cells multiply and grow uncontrollably. Cancer of the breast is a malignant growth that begins in breast cells and can spread to neighbouring tissues or even other parts of the body. Breast cancer typically begins in the cells of the lobules, which are the milk-producing glands, or the ducts, and can spread from there into the surrounding healthy breast tissue, the underarm lymph nodules, and other small organs that serve to filter out foreign substances. Lymph nodules provide a back door for cancer cells to spread to other organs. Over the past 30 years, there has been an uptick in cases of breast cancer. Somewhere between 10% and 15% of breast cancers begin in the lobules, while the remaining 50%-75% begin in the ducts. Because of improved detection methods and treatment options, the mortality rate from breast cancer has decreased in recent years. Some commonly used herbs have been officially recognised as cancer preventatives by the Cancer Research Centres. Therefore, the goal of this study is to conduct a simple, low-cost analysis of doped NPs which will kill the cancer cells and save the life of human[10-15].

Cancer nanotechnology has the potential to significantly contribute to the prevention, detection, and treatment of the disease. The ability of specific metal oxide nanoparticles (NPs) to selectively kill cancer cells while being relatively nontoxic to healthy cells has been demonstrated in an increasing number of studies. SnO NPs, in particular, had a lot of potential as a cancer treatment. SnO NPs have demonstrated inherent selective toxicity against cancer cells while posing minimal effects to the normal cells, likely as a result of their distinctive physiochemical characteristics. SnO NPs cause cancer cells to self-destruct by lowering their mitochondrial membrane potential (MMP) and releasing reactive oxygen species (ROS). It is possible to selectively damage cancer cells while causing relatively little harm to healthy cells by manipulating intracellular ROS generation. SnO NPs' potential for generating reactive oxygen species (ROS) is linked to its optical properties. Polymers doping and the synthesis of SnO-based nanocomposites are two methods that can be used to alter the optical properties of SnONPs[16-19].

SnO NPs, on the other hand, have been shown to be toxic to a variety of organisms in research. These include bacteria, microalgae, yeast, protozoa, zebrafish, and mice. That's why it's crucial to develop SnO NPs with enhanced selectivity and anticancer activity. Chitosan polymer and Co Polymer Pluronic F-127 have both shown promise as therapeutic agents. Metal oxide NPs, such as SnO_2, can have their physicochemical properties tuned with the help of chitosan and Pluronic F-127.

Hydrothermal, Sol-gel, Co-Precipitation, solvothermal, gel-combustion, microwave heating, and polyol methods have all been developed to synthesise SnO_2 Pluronic F-127 Chitosan NPs in order to take advantage of their wide range of potential uses. Producing NPs at a lower cost using any of these methods is extremely challenging and prohibitively expensive. Clearly, chemists face a formidable challenge in lowering production costs while simultaneously increasing toxicity towards target cell lines[20-25].

Scientists have begun synthesising a wide range of metal nanoparticles for use in pharmaceuticals using environmentally friendly methods to satisfy the growing demand for nanoparticles that are safe for the environment.

The environmental friendliness and use of non-hazardous solvents (typically plant extracts) in green synthesis have piqued the interest of many scientists. Plant parts like leaves, fruits, rinds, barks, seeds, and roots are mined for their extracts, which contain reducing and stabilising agents like polyphenols, flavonoids, proteins, and sugars[25-31].

Sennaauriculata (L.)Roxb. (*Cassia auriculata*, Family: Fabaceae or Leguminosae) is a common traditional and Asian beverage nutritional plant that is widely used in Indian traditional medicine for the treatment of diabetes mellitus and rheumatism. It is used in green synthesis of SnO_2Pluronic F-127 Chitosan nanoparticles[32-36].

With these considerations in mind, we prepared SnO_2-dopedPluronic F-127 chitosan nanoparticles (NPs) to enhance their anticancer potential and biocompatibility. The NPs were made using an eco-friendly process. Field emission scanning electron microscopy (FESEM), X-ray diffraction (XRD), ultraviolet-visible (UV-VIS) spectrometer, Fourier transform infrared spectroscopy (FTIR), photoluminescence (PL), and dynamic light scattering (DLS) were used to characterise the prepared samples. Antibacterial, antifungal, and anticancer Human breast cancer (MDA-MB-231) cells were used to test the properties of SnO_2-doped PF 127 Fluronic Chitosan NPs. In this study, we used breast cancer cell lines because this is the most frequently diagnosed cancer in women and the third leading cause of cancer death worldwide (after colorectal and lung cancer).

Experimental section

Collection of Plant Materials

Sennaauriculata was gathered by us in Trichy, close to the airport (coordinates: 10.7204101° N, 78.7364588° E), and then washed twice in double-distilled water. For 15 minutes, 10 grammes of finely chopped Flower was boiled in 50-60 degrees Celsius with 100 millilitres of double-distilled water. After collecting the extraction in a 250 mL Erlenmeyer flask at room temperature, it was filtered through Whatman No. 1 filter paper.

Green Synthesis

The SnO2 Pluronic F127 chitosan NPs were made using environmentally friendly techniques. The SnO2 Pluronic F127 chitosan NPs were made by mixing 100 mL of flower extract with 90 mL of 0.1M tin (II) nitrate hexahydrate (Sn (NO3)2. After ten minutes, the metal should be completely dissolved in the extract. 500 mg of chitosanwere dissolved in 50 mL of 1% acetic acid solution and 500 mg of pluronic F-127 both should be added to the extract. The concentrate yields a uniformly coloured precipitate. This solution was heated to 80° Celsius and stirred continuously for 5 hours. Drying the precipitate at 120°Celsius followed. In this way, we were able to obtain SnO_2Pluronic F127 chitosan nanopowder. Since the energy from the heat would improve the vibration and diffusion of lattice atoms for atomic rearrangement, the SnO_2Pluronic F127 chitosan NPs were annealed at 800 °C for 5 hours. The annealing process also assisted in eliminating any lingering contaminants.

Characterization Tecniques

Field emission scanning electron microscopy (FESEM), X-ray diffraction (XRD), ultraviolet-visible (UV-VIS) spectrometer, Fourier transform infrared spectroscopy (FTIR),

photoluminescence (PL), and dynamic light scattering (DLS) were all used to characterise the prepared samples.

.RESULT AND DISCUSSION

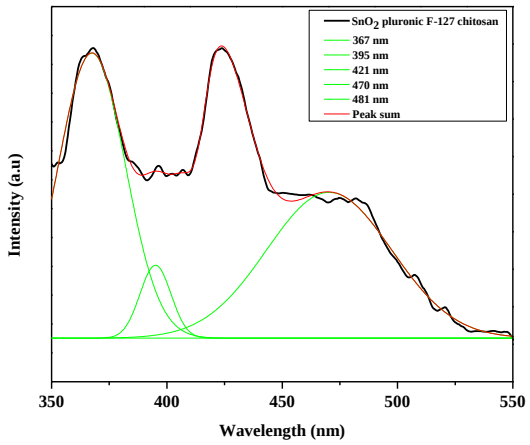

Fig 1: Shows the XRD pattern of SnO_2Pluronic F127 chitosan NPs

In order to determine the crystal structure and phase purity of the prepared SnO_2Pluronic F127 chitosan NPs, XRD (X-ray Diffraction) was used for the analysis. Reflecting planes (110), (101), (200),(211), (220), (002),(310),(112),(301),(202)and (321) have 2θ values of 26.30°, 33.60°, 37.67°, 51.52°, 54.49°, 57.58°, 61.62°, 65.66°, 71.06°, and 78.46°, as shown in Fig. 1 for chitosan (SnO_2)[37-39]. An excellent agreement was found between the positions of the diffraction patterns observed and the tetragonal rutile structure in SnO_2Pluronic F127 chitosan NPs.(JCPDS No. 01-0657). According to the Debye-Scherrer formula, the resulting powders have crystallites of size $D = \frac{0.9\,\lambda}{\beta cos\,\theta}$. K, the diffraction angle, is equal to the FWHM in radians multiplied by 0.94, where FWHM is the full width at half maximum height. The largest peaks' d values from the index are used. On average, crystals were found to be 33 nm in size.

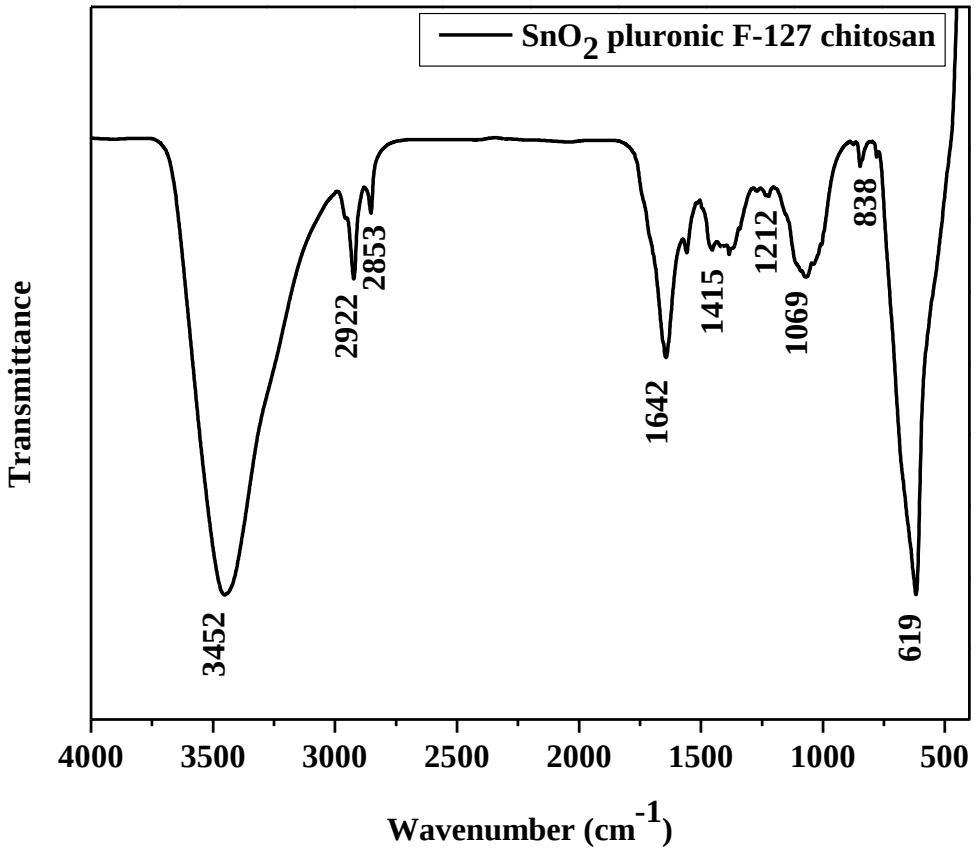

Figure 2: Shows the FTIR spectrum ofSnO_2 Pluronic F127 NPs

Molecular structure and chemical composition are typically investigated using FTIR (Fourier Transform Infrared Spectroscopy). In order to determine which chemical bonds and functional groups are present in SnO2-doped Pluronic F127 chitosan, Fourier transform infrared spectroscopy (FTIR) is employed. The water molecules absorbed on the Sno2surface cause a strong and broad O-H stretching bond at 3452cm-1.The peak at 1069 cm-1 are due to the stretching vibration of C-N and C-O confirming the presence of chitosan. The absorbance peaks at 1212 cm-1 can be assigned to the stretching vibration of chitosan main chains –C-O-C- and C-O respectively .The peaks at 1415, 2853 and 2922 cm-1 are corresponds to the stretching vibration of C-H bond and the peak at 1642 cm-1 corresponds to the stretching vibration of C=C.The C=H bending vibration of the peakPlunoric F-127 molecules is 838 cm-

[1][40-44]. Spectral peaks at 619 cm^{-1} are ascribed to anti-symmetric vibration of the Sn-O-Sn bond and symmetric vibration of the Sn-O bond, respectively.

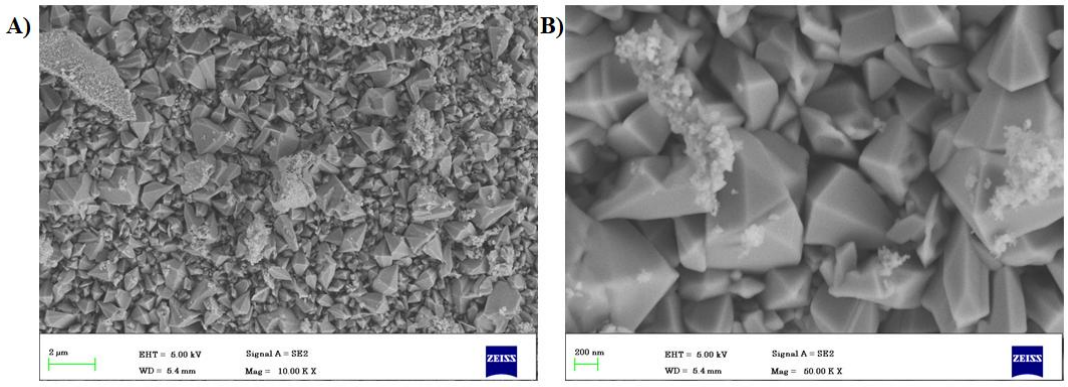

Fig 3

(A-B) Shows the Scanning electron microscopy(SEM) Images of SnO2 Pluronic F127 Chitosan

The morphologies of SnO_2PluronicF127 Chitosan were analysed using scanning electron microscopy (SEM). The low-magnification SEM image in Fig.3 (A) reveals that SnO2 is made up of particles with a cube-shaped and elliptical structure and a diameter of 29-39 nm. In order to better comprehend the structural characteristics of SnO_2Pluronic F127 Chitosan, high-magnification SEM images were analysed (Fig.3(B)). SnO_2Pluronic F127 Chiosan particles have nanoparticles on their surface that range in size from several nanometers to one nanometer[45-47]. In addition, a few microspheres with a minuscule elongated form were visible through the crevices in other particles. Chiosan and Pluronic F127 could influence the assembly pattern of SnO_2 nanoparticles.

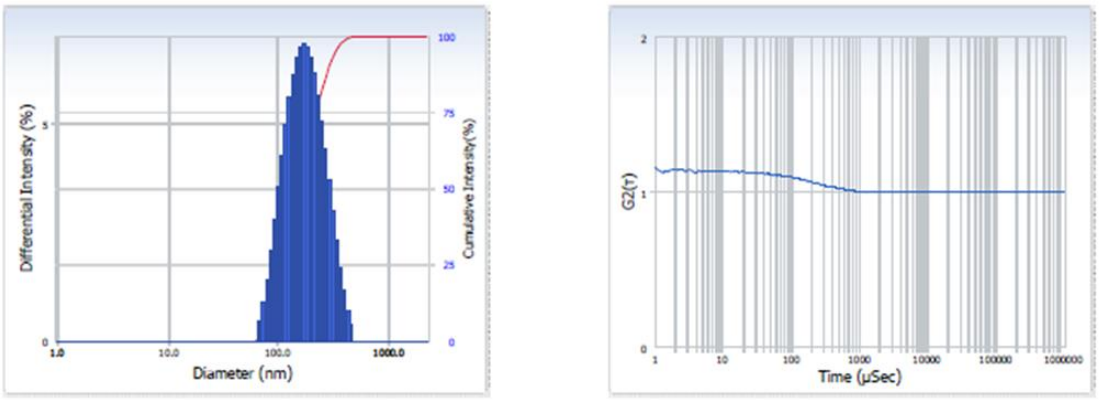

Fig 4 (DLS) dynamic light scattering of Sno_2Pluronic F127 Chiosan NPs

The particles in a watery solution were analysed for their dimension shipping using the technique of dynamic light scattering (DLS). DLS measurements demonstrated a rise in the dimension of Sno_2Pluronic F127 Chiosan NPs, which were determined to be 169 nm, accordingly (nanoparticle itself, surrounded by water molecules). This happened due to the simple fact that liquid molecules that are completely covered the Sno2 Pluronic F127 Chitosan NPs, dictating their hydrodynamic size. The growth and nucleation rate of the SnO NPs were impeded by extraneous foreign substances like Pluronic F127 and Chitosan, resulting in a smaller particle size[48].

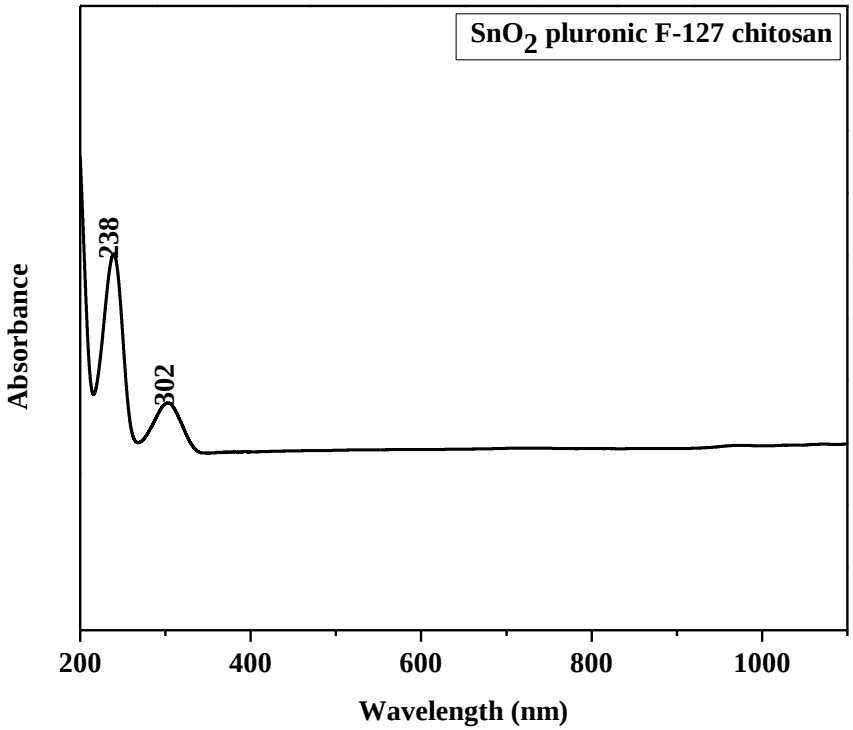

Fig 5 UV-visible absorption by SnO_2Pluronic F127 Chiosan nanoparticles

The spectrum of UV-visible absorption by SnO_2Pluronic F127 Chiosannanoparticles is depicted in the figure. The range of the UV spectrum was 190-1100 nm. A UV-Vis spectrophotometer is a useful tool for evaluating the optical properties of SnO_2PEG NPs, which are proportional to the size of the SnO_2Pluronic F127 ChiosanNPs. Variation in the size of SnO_2Pluronic F127 ChiosanNPs causes a change in the position of the absorption band or the surface Plasmon resonance band. The absorption edge is predicted to move to a higher energy as the particle size decreases due to the quantum confinement effect. This new study lends further credence to the previous findings. Absorption maxima are observed at 238 and 304 nm for SnO_2Pluronic F127 ChiosanNPs[49].

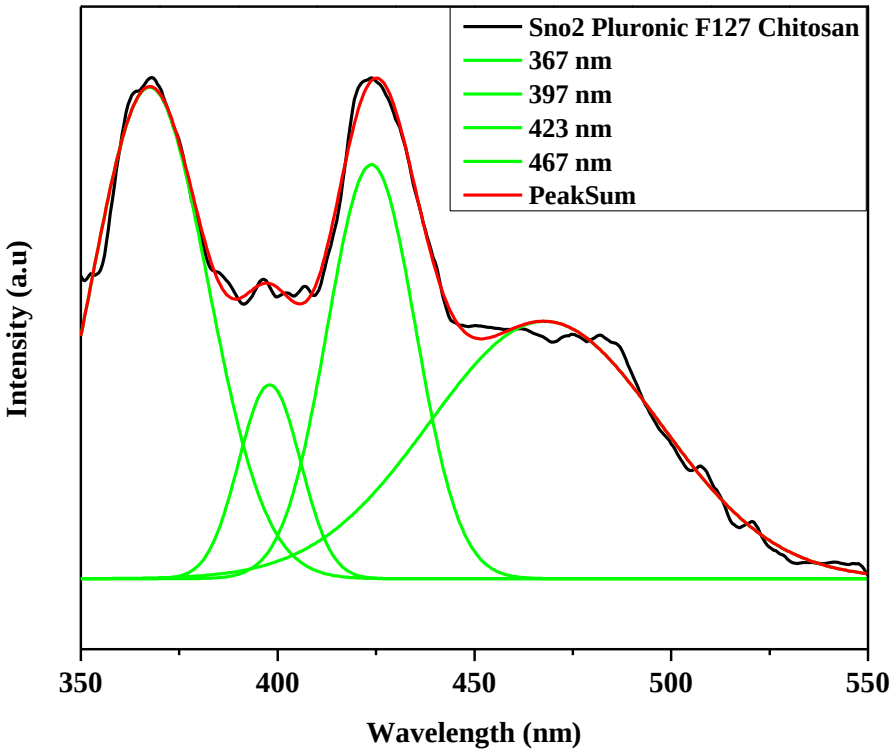

Fig 6 photoluminescence spectra of the Sno_2Pluronic F127 Chitosan

On display in the figure are the photoluminescence spectra of the Sno2 Pluronic F127 Chitosan NPs, which were excited at a wavelength of 325 nm. The optical properties of all of the nanoparticles demonstrate that the peak locations of their spectra are extremely identical to one another across the entire spectrum of wavelengths. This is demonstrated by the fact that the peak positions are very similar. The emission peaks associated with Sno2 Pluronic F127 Chitosan NPs were observed to be located at (367,397,423 and 467) nm, respectively. The movement of an electron from a shallow donor level of natural Sn interstitials to the top level of the valence band is what causes the violet emission centre at 423 nm for the Sno_2Pluronic F127 Chitosan NPs. This transition takes place when an electron moves from a shallow donor level to the top level. It is at a wavelength of 423 nm that this transition takes place. This transition takes place as the electron moves farther away from a naturally

occurring Sn interstitial. The wavelengths of 452 and 483 nm, respectively, are where the blue emission peaks for Sno_2Pluronic F127 Chitosan NPs can be found[50].

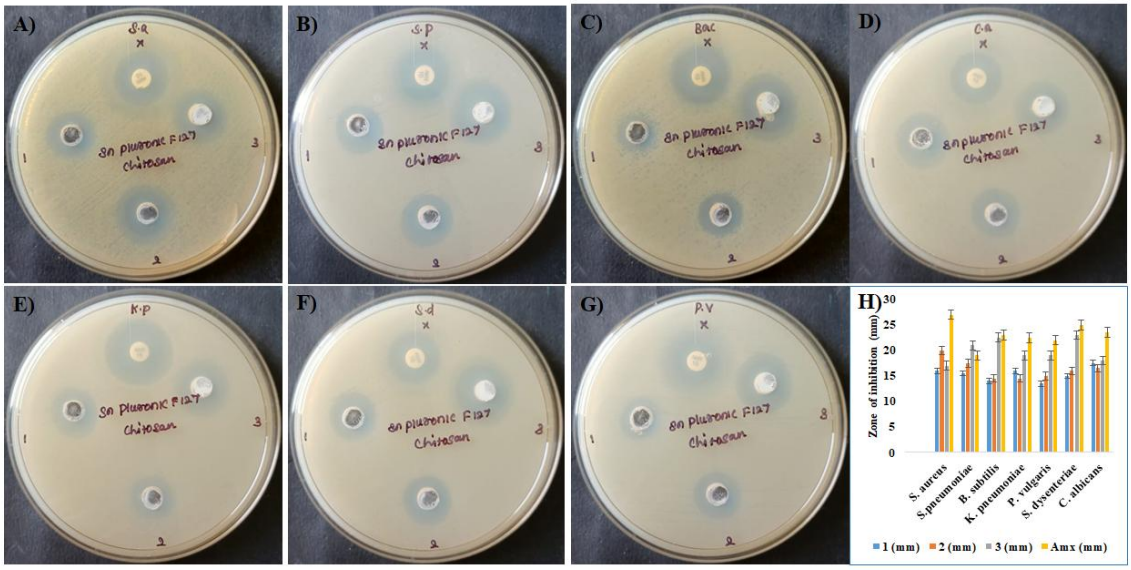

FIG:7Antibacterial and Anti-fungal zone of inhibition (A-G) and Graph of Antibacterial and Antifungal Activity (H) for the prepared Sno_2Pluronic F127 Chitosan

We retested the antibacterial effects of amoxicillin and Sno_2Pluronic F127 Chitosan NPs against various strains of *Staphylococcus aureus, Klebsiellapneumoniae, Shigelladysenteriae, Pneumocystis jirovecii, Bacillus megaterium,* and *Proteus valgaris* using the well-diffusion method. Gram-positive bacterial culture is more active than gram-negative bacterial culture. This is due to the fact that the cell wall structure of gram-positive bacteria is completely different from that of gram-negative bacteria, which is why gram-positive cultures produce more activity. Gram-positive bacteria are protected from outside threats by their cell walls, which are made up of multiple layers of a substance called peptidoglycan.Teichoic and lipoteichoic acids, in addition to surface proteins, are both examples of polymers that can be fixed by the peptidoglycan. Gram-negative bacteria have an additional outer membrane on

their cell walls that is composed of porins, a thin peptidoglycan layer, and lipopolysaccharide (LPS). Because of this, the exterior membrane of Gram-negative bacteria makes it difficult for the SnO to murder the cell. This is the reason why SnO NP has a better effect on Gram-positive bacteria than it does on Gram-negative bacteria.According to the findings of the XRD analysis, the NPs in the sample of Sno_2Pluronic F127 Chitosan had an average size of 32 nm. There is a possibility that smaller NP are more toxic than larger NP because more particles are required to cover the surface of the bacteria and generate more ROS, which are produced by SnO on the surface of the cells. The fact that smaller NP are able to permeate the bacterial membrane more easily than larger NP is suggestive of the fact that the antibacterial action is dependent on the size of the SnO NPs. This is because of the high interfacial area of the smaller NP[51].

The biologically synthesised Sno_2Pluronic F127 Sodium Alginate is put through tests for both its antibacterial and antifungal properties using the well diffusion method. The candida overgrowth known as Candida albicans can be treated with Sno_2Pluronic F127Chitosan.According to the diameter of the inhibition zone that was calculated, the doped nanomaterial Sno_2Pluronic F127 Chitosan possesses antifungal activity that is superior to that of SnO NPs. *Sennaauriculata* possesses antifungal properties, and these properties have the potential to enhance the antifungal efficacy of Sno_2Pluronic F127 Sodium Alginate that is manufactured through biological means.

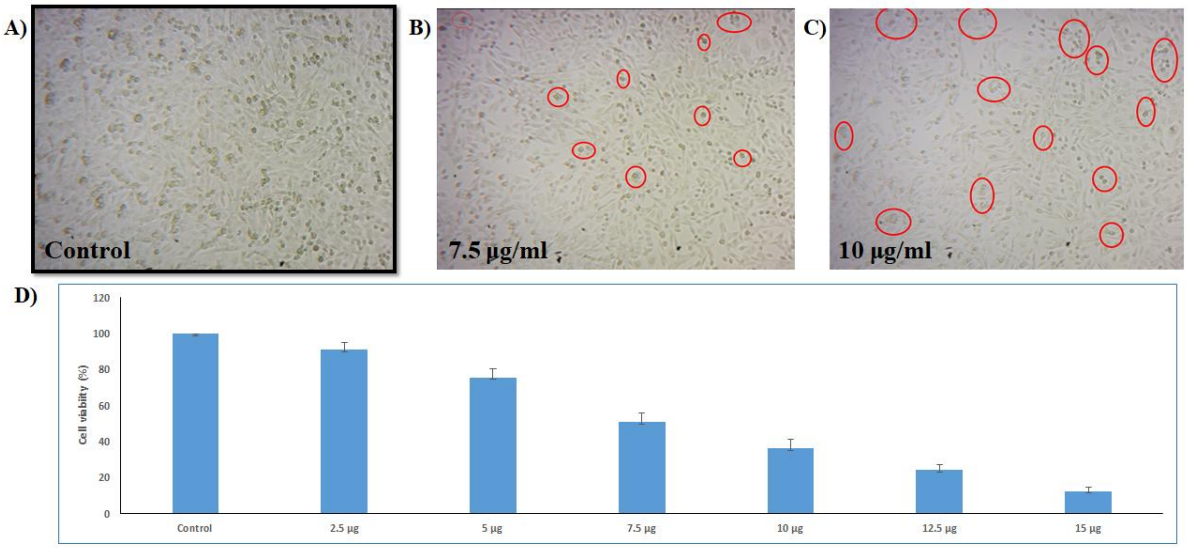

Fig 8: Morphological changes in control (A) and Sno_2Pluronic F127 Chitosan (B-C)treated Breast cancer (MDA-MB-231) cells for 24 h. (D) Graphical presentation of Control and treated cells.

The anticancer activity of a sample of Sno_2Pluronic F127 Chitosan is displayed in Fig. by making use of the MDA-MB-237 human breast cancer cell line. The Sno_2Pluronic F127 Chitosan NPs were subjected to an incubation period of twenty-four hours at concentrations ranging from 0 to 15µg/ml, with the latter showing an IC_{50} value of 7.5 µg/mlfor cytotoxicity.

There are a number of factors that can influence the cytotoxicity of nanomaterials, including their size, dissolution rate, surface defects (oxygen vacancies), and production of reactive oxygen species (ROS). The blue emission peak that can be seen in the PL spectrum (this work) is attributed to oxygen vacancies (Ov) in Sno2 Pluronic F127 Chitosan. This peak can be found anywhere between 0 and 480 nanometers. This is due to the high levels of reactive oxygen species (ROS), also known as radicals, that are produced[52-53]. Cancer cells were exposed to a very high degree of oxidative stress, which occurs as a result of the production

of reactive oxygen species (ROS; OH, H_2O_2 and O_2) and how they interact with macro molecules (DNA, lipids, and proteins).

Conclusion

In this study, the cytotoxicity of Sno_2Pluronic F127 Chitosan NPs was tested against both gram-negative and gram-positive bacteria, as well as cancer-induced cells. *Sennaauriculata* leaf extracts were used in a green precipitation process to create Sno_2 Pluronic F127 Chitosan NPs. XRD analysis verified that Sno_2Pluronic F127 Chitosan NPs have a Tetragonal rutile and an average size of 33nm.SEM image reveals that SnO_2 is made up of particles with a cube-shaped and elliptical structure and a diameter of 29-39 nm. FTIR spectra demonstrate that the formation of Pluronic F127 and Chitosan with SnO NPs coincides with the formation of strong higher intermolecular hydrogen bonds within the material matrix. Tin vacancies, oxygen vacuoles, and surface flaws were found to influence the band emission of Sno_2Pluronic F127 Chitosan NPs, as determined by PL analysis. Sno_2Pluronic F127 Chitosan NPs were found to be more effective at killing bacteria in lab tests than the commonly used antibiotic amoxicillin. Sno_2Pluronic F127 Chitosan NPs were unable to kill the human breast cancer cell line, as they had done with other cancer cell lines. Overall, the results show that the synthesised Sno_2Pluronic F127 Chitosan NPs have potent antibacterial and anticancer effects against the bacterial strains and cancer cell lines used in the studies.

Author Contributions:

Mrs.PP carried out the preparation of the nanoparticles and executes the physical characterization studies and contributed to the main text of the manuscript. Dr.AS checked the scientific information and flow of the text to maintain a better readability. Further this research work is not funded by any agency.

Compliance with ethical standards:

Conflict of interest: The author declared that they have no conflict of interest

Reference

1. Sung H, Ferlay J, Siegel RL, Laversanne M, Soerjomataram I, Jemal A, et al. Global cancer statistics 2020:GLOBOCAN estimates of incidence and mortality worldwide for 36 cancers in 185 countries. CA Cancer J Clin 2021;71:209–49.
2. Ferlay J, Ervik M, Lam F, Colombet M, Mery L, Piñeros M, et al. Global cancer observatory:Cancer today. Lyon, France: International Agency for Research on Cancer;2020 Available from:https://gco.iarc.fr/today accessed on August 5, 2022.
3. Ahamed, Maqusood, MohdJavedAkhtar, MA Majeed Khan, and Hisham A. Alhadlaq. "SnO2-doped ZnO/reduced graphene oxide nanocomposites: synthesis, characterization, and improved anticancer activity via oxidative stress pathway." International journal of nanomedicine 16 (2021): 89.
4. Tammina, Sai Kumar, Badal Kumar Mandal, ShivenduRanjan, and NanditaDasgupta. "Cytotoxicity study of Piper nigrum seed mediated synthesized SnO2nanoparticles towards colorectal (HCT116) and lung cancer (A549) celllines." Journal of Photochemistry and Photobiology B: Biology 166 (2017): 158-168.

5. M.D. Arienzo, D. Cristofori, R. Scotti and F. Morazzoni, New insight into the SnO2sensing mechanism based on the properties of shape controlled tin oxidenanoparticles, Chem. Mater. 25, 2013, 3675-3686.
6. A.M. Al-Hamdi, M. Sillanpaa, J. Dutta, Photocatalytic degradation of phenol byiodine doped tin oxide nanoparticles under UV and sunlight irradiation, J. Alloy.Compd. 618, 2015, 366-371.
7. H. Yang, G. Yu, H. Liu, Synthesis of 3D flower like SnO2 with hierarchicalnanostructures and high reversible capacity as lithium ion battery anode, J. Electron.Mater. 44, 10, 2015, 3744-3751.
8. M.M. Kumari, D. Philip, Synthesis of biogenic SnO2 nanoparticles and evaluation ofthermal, rheological, antibacterial and antioxidant activities, Powder Technol. 270,2015, 312-319.
9. V.K. Vidhu, D. Philip, Biogenic synthesis of SnO2 nanoparticles Evaluation ofantibacterial and antioxidant activities, Spectro. Chim. ActaA 134, 2015, 372-379.
10. Wiesmann N, Tremel W, Brieger J. Zinc oxide nanoparticles for therapeutic purposes in cancer medicine. J Mater Chem B. 2020;8(23):4973–4989. doi: 10.1039/d0tb00739k
11. Z. Hu, Y. Xie, Y. Wang, L. Mo, Y. Yang, Z. Zhang, Polyaniline/SnO2 nanocompositefor super capacitor applications, Mater. Chem. Phys. 114, 2009, 990-995.
12. H. Chen, S.Y. Ma, W.X. Jin, W.Q. Li, The mode of multi-tier nested Tin dioxidepolyhedral nanoparticles with exposed high-energy facets and their gas sensingproperties, Mater. Lett. 164, 2016, 627-630.

13. H. Kose, S. Karaal, A.O. Aydin, H. Akbulut, Structural properties of size-controlledSnO2 nanopowders produced by sol–gel method Mat. Sci. Semico. Proc. 38, 2015,404-412.
14. V. Agrahari, M.C. Mathpal, M. Kumar, A. Agarwal, Investigations of optoelectronicproperties in DMS SnO2 nanoparticles, J. Alloy. Compd. 622, 2015, 48-53.
15. Lu, Ming-Pei, Jinhui Song, Ming-Yen Lu, Min-Teng Chen, YifanGao, Lih-JuannChen, and Zhong Lin Wang. "Piezoelectricnanogenerator using p-type ZnO nanowirearrays." Nano letters 9, no. 3 (2009): 1223-1227.
16. Ann, Ling Chuo, Shahrom Mahmud, SitiKhadijahMohdBakhori, AmnaSirelkhatim,DasmawatiMohamad, HabsahHasan, AzmanSeeni, and Rosliza Abdul Rahman."Antibacterial responses of zinc oxide structures against Staphylococcus aureus,Pseudomonas aeruginosa and Streptococcus pyogenes." Ceramics International 40,no. 2 (2014): 2993-3001.
17. Salehi, Raziyeh, MokhtarArami, Niyaz Mohammad Mahmoodi, HajirBahrami, andShookaKhorramfar. "Novel biocompatible composite (chitosan–zinc oxidenanoparticle): preparation, characterization and dye adsorption properties." Colloidsand Surfaces B: Biointerfaces 80, no. 1 (2010): 86-93.
18. Raoufi, Davood. "Synthesis and microstructural properties of ZnO nanoparticlesprepared by precipitation method." Renewable Energy 50 (2013): 932-937.
19. Ma, Jianzhong, Junli Liu, Yan Bao, Zhenfeng Zhu, Xiaofeng Wang, and Jing Zhang."Synthesis of large-scale uniform mulberry-like ZnO particles with microwavehydrothermal method and its antibacterial property." Ceramics International 39, no. 3(2013): 2803-2810.

20. Taha, M. O., K. M. Aiedeh, Y. Al-Hiari, and H. Al-Khatib. "Synthesis of zinc-crosslinkedthiolatedalginic acid beads and their in vitro evaluation as potentialenteric delivery system with folic acid as model drug." Die Pharmazie-AnInternational Journal of Pharmaceutical Sciences 60, no. 10 (2005): 736-742.
21. Layek, Rama K., Md Elias Uddin, Nam Hoon Kim, Alan Kin Tak Lau, and JoongHeeLee. "Noncovalent functionalization of reduced graphene oxide with pluronic F127and its nanocomposites with gum Arabic." Composites Part B: Engineering 128(2017): 155-163.
22. Soldano C, Mahmood A, Dujardin E. Production, properties and potential ofgraphene. Carbon 2010; 48: 2127- 50.Kim YJ, Kim Y, Novoselov K, Hong BH. Engineering electrical properties ofgraphene: chemical approaches. 2D Mater 2015; 2: 042001(1)-042001(17).
23. Neto AHC, Guinea F, Peres NMR, Novoselov KS, Geim AK. The electronicproperties of graphene. Rev Mod Phys 2009; 81: 109-61.
24. Kim H, Miura Y, Macosko CW. Graphene/polyurethane nanocomposites for improvedgas barrier and electrical conductivity. Chem Mater 2010; 22 :3441–50.
25. Srivastava M; Uddin ME; Singh J; Kim NH ; Lee JH. Preparation andcharacterization of self-assembled layer by layer NiCo2O4-reduced graphene oxidenanocomposite with improved electrocatalytic properties. Journal of Alloys andCompounds 2013; 590: 266- 276.
26. Bandyopadhyay P, Nguyen TT, Li X, Kim NH, Lee JH. Enhanced hydrogen gasbarrier performance of diaminoalkane functionalized stitched grapheme oxide/polyurethane composites. Composites Part B: Engineering 2017; 117: 101-10.

27. Gopalsamy K, Balamurugan J, Thanh TD, Kim NH, Hui D, Lee JH. Surfactant-freesynthesis of NiPdnanoalloy/graphenebifunctionalnanocomposite for fuel cell.Composites Part B: Engineering 2017; 114: 319-27.

28. Liu H, Bandyopadhyay P, Kshetri T, Kim NH, Ku BC, Moon B, Lee JH. Layer-by-layer assembled polyelectrolyte-decorated graphene multilayer film for hydrogen gasbarrier application. Composites Part B: Engineering 2017; 114: 339-47.
29. Shen HS, Xiang Y, Lin F, Hui D. Buckling and postbuckling of functionally gradedgraphene-reinforced composite laminated plates in thermal environments. CompositesPart B: Engineering 2017; 119: 67-78.
30. Park WB, Bandyopadhyay P, Nguyen TT, Kuila T, Kim NH, Lee JH. Effect of highmolecular weight polyethyleneimine functionalized graphene oxide coatedpolyethylene
31. Prasathkumar, Murugan, Kannan Raja, Krishnan Vasanth, AmeerKhusro,SubramaniamSadhasivam, Muhammad Umar KhayamSahibzada, Mohamed RagabAbdel Gawwad, Dunia A. Al Farraj, and Mohamed S. Elshikh. "Phytochemicalscreening and in vitro antibacterial, antioxidant, anti-inflammatory, anti-diabetic, andwound healing attributes of Sennaauriculata (L.) Roxb. leaves." Arabian Journal ofChemistry 14, no. 9 (2021): 103345.
32. Shanmugasundaram, R., K. V. Devi, T. P. Soris, A. Maruthupandian, and V. R.Mohan. "Antidiabetic, antihyperlipidaemic and antioxidant activity of Sennaauriculata (L.) Roxb. leaves in alloxan induced diabetic rats." Int J Pharm Tech Res 3,no. 2 (2011): 747-56.

33. Srinivasulu, Dasaiah. "Sennaauriculata L. flower petal biomass: An alternative greenbiosorbent for the removal of fluoride from aqueous solutions." ActaEcologicaSinica (2021).
34. Chandrasekaran, Senthilkumar, VenkattappanAnbazhagan, and ShanmugamAnusuya. "Green route synthesis of ZnO nanoparticles using Sennaauriculataaqueous flower extract as reducing agent and evaluation of its antimicrobial,antidiabetic and cytotoxic activity." Applied Biochemistry and Biotechnology (2022):1-15.
35. T. Sun, Y.S. Zhang, B. Pang, D.C. Hyun, M. Yang, Y. Xia, Engineered nanoparticlesfor drug delivery in cancer therapy, Angew. Chem., 53, 2014, 12320–12364.
36. J.S. Butler, P.J. Sadler, Targeted delivery of platinum-based anticancer complexes,Curr. Opin. Chem. Biol. 17, 2013, 175–188.
37. K. Li, Y. Jiang, D. Ding, X. Zhang, Y. Liu, J. Hua, S. Feng, B. Liu, Folicacidfunctionalized two-photon absorbing nanoparticles for targeted MCF-7 cancercell imaging, Chem. Commun., 47, 2011, 7323–7325.
38. O.V. Salata, Applications of nanoparticles in biology and medicine, J.Nanobiotechnol. 2, 2004, 1-6.
39. S.M. Roopan , S.H.S. Kumar, G. Madhumitha, K. Suthindhiran, Biogenic-Production of SnO2 Nanoparticles and Its Cytotoxic Effect Against HepatocellularCarcinoma Cell Line (HepG2), Appl. Biochem. Biotechnol. 175, 2015, 1567–1575.
40. P.J. Shiny, A. Mukherjee, N. Chandrasekaran, DNA damage and mitochondria-mediated apoptosis of A549 lung carcinoma cells induced by biosynthesised silverand platinum nanoparticles, RSC Adv., 6, 2016, 27775-27787.

41. N. Pandey, S. Dhiman, T. Srivastava , S. Majumder, Transition metal oxidenanoparticles are effective in inhibiting lung cancer cell survival in the hypoxic tumormicroenvironment, Chem-Biol. Interact 254, 2016, 221-230.
42. V. E. Rivera. M.U. Ramirez, S.G. Pozos, S. Velumani, L.A. Mendoza, A.D.V. Ruiz,Cytotoxicity of semiconductor nanoparticles in A549 cells is attributable to theirintrinsic oxidant activity, J. Nanopart. Res. 85, 2016, 1-12.
43. Garrafa-Galvez, H. E., O. Nava, C. A. Soto-Robles, A. R. Vilchis-Nestor, A. Castro-Beltrán, and P. A. Luque. "Green synthesis of SnO2 nanoparticle using Lycopersiconesculentum peel extract." Journal of Molecular Structure 1197 (2019): 354-360.
44. Amara, Chedia Ben, NoushinEghbal, Nadia Oulahal, Pascal Degraeve, and AdemGharsallaoui. "Properties of lysozyme/sodium alginate complexes for the
45. development of antimicrobial films." Food Research International 89 (2016): 272-280.
46. Raslan, R., and A. W. Mohammad. "Polysulfone/Pluronic F127 Blend UltrafiltrationMembranes: Preparation and." Journal of Applied Sciences 10, no. 21 (2010): 2628-2632.
47. Ahmadabad, Leila Ebrahimi, FiroozehSamiaKalantari, Hui Liu, AnwarulHasan,NiushaAbbasiGamasaee, ZehraEdis, Farnoosh Attar et al. "Hydrothermal method-based synthesized tin oxide nanoparticles: Albumin binding and antiproliferativeactivity against K562 cells." Materials Science and Engineering: C 119 (2021):111649.
48. APS, GAHLOT, R. Pandey, S. Singhania, A. Garg, and P. Gupta. "Evolution of tinoxide (SnO2) nanostructures synthesized by hydrothermal method." (2021).

49. Cai, Zicheng, Eunjung Goo, and Sunghoon Park. "Synthesis of tin dioxide (SnO2)hollownanospheres and its ethanol-sensing performance augmented by goldnanoparticle decoration." Journal of Alloys and Compounds 883 (2021): 160868.
50. Gahlot, Ajay Pratap Singh, RupaliPandey, SandeepSinghania, AmitGarg, andMridula Gupta. "Evolution of tin oxide (SnO2) nanostructures synthesized byhydrothermal method." (2021).
51. Kong, Xingang, Jiarui Zhang, Jianfeng Huang, Jiayin Li, Yi Qin, Ting Zhao, and QiFeng. "Microwave assisted hydrothermal synthesis of tin niobatesnanosheets withhigh cycle stability as lithium-ion battery anodes." Chinese Chemical Letters 30, no. 3(2019): 771-774.
52. Mishra, SoumyaRanjan, and MdAhmaruzzaman. "Tin oxide based nanostructuredmaterials: synthesis and potential applications." Nanoscale (2022).
53. Etminan, Majid, GholamrezaNabiyouni, and DavoodGhanbari. "Preparation of tinferrite–tin oxide by hydrothermal, precipitation and auto-combustion: photo-catalystand magnetic nanocomposites for degradation of toxic azo-dyes." Journal of MaterialsScience: Materials in Electronics 29, no. 3 (2018): 1766-1776.